BER Analysis of Optical Wireless Signals through Lognormal Fading Channels with Perfect CSI

Hassan Moradi, Maryam Falahpour, Hazem H. Refai
Electrical and Computer Engineering
University of Oklahoma
Tulsa, OK, USA
{hmoradi, maryam, hazem}@ou.edu

Peter G. LoPresti
Electrical Engineering
University of Tulsa
Tulsa, OK, USA
pgl@ohm.ee.utulsa.edu

Mohammed Atiquzzaman
Computer Science
University of Oklahoma
Norman, OK, USA
atiq@ou.edu

***Abstract*— Due to inconsistent atmospheric conditions, scattering and scintillation of free space optical (FSO) signal can occur, thus negatively influencing the received signal intensity. The channel is usually modeled as a normalized fading coefficient with additive Gaussian noise. Optimal detection of the received signal is designed based on a decision rule, e.g., *Maximum Likelihood* (ML), assuming the receiver knows the noise statistics and fading correlation of the channel. This paper briefly deals with analysis on bit error rate (BER) of a wireless optical signal passing through a lognormally distributed fading channel, when perfect knowledge of channel state information (CSI) at the receiver side is available. Two approaches will be presented to provide closed-form expressions for BER. One uses Gauss–Hermite quadrature approximation and the other one is based on power series. While numerical analysis shows a very small approximation error when the Gauss–Hermite approach is considered, the power series approach does not uses any approximation.**

***Keywords: FSO, Channel state information (CSI), BER, Lognormal fading, Gauss–Hermite quadrature, Power series, Approximation error*.**

I. INTRODUCTION

There are various types of undesired noises in wireless optical, i.e. FSO, channels which adversely affect the BER performance of a communication link. Background noise, dark noise and thermal noise are among the most common noises which are all modeled as an additive Gaussian noise with zero or even non-zero mean [1]. The design and practical implementation of optimal detector, commonly based on ML function, is as simple as will be described here later. In this case a simple closed form expression can be derived.

Although the additive noise degrades the performance of the link in terms of bit error, it is not the only random variable that affects the FSO channel. Like any wireless communication link, the FSO channel faces fading of the signal due to propagation in free space. The fading comes from the atmosphere induced turbulence as scintillation which is different than the visibility considerations due to fog and Mie scattering which deals with signal attenuation, previously investigated in [2] and [3]. The fading random variable is usually modeled as a lognormal [4], Gamma [5] or Gamma-Gamma [6-7] distribution model in literature. The fading not only decreases significantly the BER performance of the communication link, but it increases the complexities of designing appropriate receiver based on optimal detection [8].

In this paper, we apply a lognormal fading to the system model and mathematically investigate the channel bit error rate in the case of perfect channel state information. It means that the receiver has the information about the instantaneous value of fading coefficient for each symbol. Thus, the receiver does not require the estimation of the channel to mitigate the effect of the fading on signal. In this case, the ML–based detection metric can be simply designed as simple as a detector of Gaussian channel. But as mentioned earlier, the BER performance is still affected by the turbulence induced fading. We assume an on-off keying (OOK) modulation format at the transmitter and direct (incoherent) detection at the receiver side. No intersymbol interference in considered through the discussions in this paper.

In Section II we define the system model. Section III provides the BER calculation, where two approaches are applied here to derive closed-form expression for BER in a lognormally faded channel. One is the power series approach which provides an exact expression while the second is based on the help of Gauss–Hermite quadrature which was previously studied in [4]. But here we analyze the approximation error if the Gauss–Hermite is used. In Section IV we briefly present the numerical simulations based on derived equations. Finally, a brief conclusion will be presented in Section V.

II. CHANNEL MODEL

A. Modulation and Additive Noise

The received signal $i_d(t)$ by OOK modulation can be expressed by

$$i_d(t) = h(t)s(t) + i_n(t) \tag{1}$$

where $s(t) \in \{0,1\}$ is the transmitted signal; $h(t)$ is the normalized channel fading intensity due to atmospheric turbulence and considered to be constant over a large number of transmitted bits; and $i_n(t)$ is total additive noise. For simplicity, investigators neglect term time (t) in the analysis presented herein. Although non-random attenuation due to propagation and scattering can be also included in the model [2], [3], it does not affect the results when communication is stochastically analyzed.

Assuming the channel is not effected by turbulence-induced fading, i_n will be the only random variable used in the model.

978-1-4244-5247-7/09/$26.00 ©2009 IEEE

The averaged ML-based bit error rate for such a Gaussian channel with equally likely transmitted bits is expressed in terms of noise and signal parameters σ_1, σ_0 and P_t:

$$P_{e,G}(\sigma_1, \sigma_0, P_t) = \frac{1}{2} erfc\left(\frac{\sqrt{2}RP_t}{\sigma_1 + \sigma_0}\right) \quad (2)$$

where σ_1 and σ_0 are the standard deviations of the noise currents for symbols '1' and '0', respectively, and where they are assumed to be different [9]. In (2) R is the receiver's responsivity, i.e. optical-to-electrical conversion coefficient; P_t is the average of transmitted power; and *erfc*(.) is the *complementary error function*. For simplicity, we can assume $2P_tR = 1$. This minimal error probability is provided by the ML-based decision threshold expressed by [9]

$$I_{D,G} = \frac{\sigma_0 I_1 + \sigma_1 I_0}{\sigma_0 + \sigma_1} \quad (3)$$

that can be assumed constant for a given observation period. In (3) $I_1 (= I_0 + 2P_tR)$ and I_0 are averages of the generated currents at the receiver for symbols '1' and '0', respectively. Additional details about noise parameters can be found in [9]. Note that for an FSO channel with only additive Gaussian noise, the average SNR can be expressed by [1]

$$\gamma_G = \frac{4R^2 P_t^2}{(\sigma_1 + \sigma_0)^2} \quad (4)$$

Then BER can be expressed in terms of the average SNR

$$P_{e,G}(\gamma_G) = \frac{1}{2} erfc\left(\sqrt{\frac{\gamma_G}{2}}\right) \quad (5)$$

B. Distribution of Fading Intensity

A random variable B has a lognormal distribution if the random variable A=ln$B$ has a normal (i.e., Gaussian) distribution. So, if the amplitude of the random path gain B is I, the optical intensity $I=B^2$ is also lognormally distributed in this case. Consequently, The fading channel coefficient, which models the channel from the transmit aperture to the receive aperture, is given by

$$h = \frac{I}{I_m} = e^{2X} \quad (6)$$

in which I_m is the signal light intensity, actually at the transmitter, without turbulence; I is the signal light intensity, actually at the receiver, with turbulence; and log-amplitude X is the identically distributed normal random variable with mean μ_x and standard deviation σ_x:

$$f_x(X) = \frac{1}{\sqrt{2\pi}\sigma_x} \exp\left(-\frac{(X - \mu_x)^2}{2\sigma_x^2}\right) \quad (7)$$

Substituting (6) in (7), the distribution of light intensity fading induced by turbulence is a log-normal distribution, which is expressed by

$$f_I(h) = \frac{1}{\sqrt{8\pi} h \sigma_x} \exp\left(-\frac{[\ln(h) - 2\mu_x]^2}{8\sigma_x^2}\right) \quad (8)$$

where $h \geq 0$ from (6). Note that the change of variables introduces an additional $1/2h$ term outside of the exponential term from the fact $dx = (1/2h)\, dh$.

C. Mean and Variance

Since variable X is Gaussian, Eq. (6) denotes that the expected value of the channel coefficient h is equal to Gaussian *moment-generating function* (MFG) of X at point 2

$$\mu_I = E[h] = \mathcal{M}_x(2) = e^{(2\mu_x + 2\sigma_x^2)} \quad (9)$$

Assuming the channel coefficients at different times are independent, the variance of h can be calculated as

$$\sigma_I^2 = E[h^2] - E[h]^2 \quad (10)$$
$$= \mathcal{M}_x(4) - (\mathcal{M}_x(2))^2 = e^{(4\mu_x + 4\sigma_x^2)}(e^{4\sigma_x^2} - 1)$$

D. Normalized Fading

In scintillation fading with scintillation index *S.I.*, we can generate average power loss due to atmospheric fading unity, such that the fading does not, on average, attenuate or amplify the optical power. We choose

$$\mu_I = 1 \quad (11)$$

that leads us to $\mu_x = -\sigma_x^2$. Thus, the variance will be equal to

$$\sigma_I^2 = e^{4\sigma_x^2} - 1 \quad (12)$$

This parameter is the so called *scintillation index*, S.I. It can be seen from (12) that the parameter σ_x is different from the fading standard deviation. Authors refer to σ_x as *fading intensity* in this paper. Finally, the lognormal distribution in (8) will be given by

$$f_I(h) = \frac{1}{\sqrt{8\pi} h \sigma_x} \exp\left(-\frac{[\ln(h) + 2\sigma_x^2]^2}{8\sigma_x^2}\right) \quad (13)$$

in which σ_x is defined as

$$\sigma_x = \frac{\sqrt{\ln(S.I. + 1)}}{2} \quad (14)$$

Note that for a lognormal channel with additive Gaussian noise, the instantaneous SNR from (4) will be converted to

$$\gamma_L = \frac{4h^2 R^2 P_t^2}{(\sigma_1 + \sigma_0)^2} \quad (15)$$

Note that for a lognormal channel with additive Gaussian noise, the instant SNR from (4) will be converted to

E. Channel State Information (CSI)

CSI is the realization of the *instantaneous* fading state, i.e. fading coefficients h, at each symbol period. Some investigations assume perfect availability of CSI at the receiver [5], [10]. This assumption enables the design of the optimal detector in its simplest form so that the ML-based decision threshold is defined simply as

$$I_{D,\,With-CSI} = \frac{\sigma_0 (I_0 + 2P_tRh) + \sigma_1 I_0}{\sigma_0 + \sigma_1} \quad (16)$$

Detection takes place by the computation of (16) for any individually received symbol r, when h is known at the receiver side. A BER analysis will be presented in the following section.

That the receiver has no knowledge of the instantaneous fading state will be discussed in subsequent sections.

III. BER Calculation

A closed form expression for the probability of error for a strong atmospheric-induced turbulence fading channel with Gamma distribution and perfect CSI was presented in [5]. We extend it for a *Gamma-Gamma* distribution which will be

$$P_{e,Gamma-Gamma}(\gamma_G,\alpha,\beta)=$$
$$\frac{2^{\alpha\beta-2}}{\sqrt{\pi^3}\Gamma(\alpha)\Gamma(\beta)}G^{2,4}_{5,2}\left[\frac{\gamma_G}{\alpha^2\beta^2}\left|\begin{matrix}1-\frac{\alpha+\beta}{2},\ 2-\frac{\alpha-\beta}{2},\ 0,\frac{1}{2},1\\ 0,\ \frac{1}{2}\end{matrix}\right.\right] \quad (17)$$

The approaches presented in this section are initiated to find expressions computationally simplified to achieve real-time error analyses of BER in *lognormal* channels. In the presence of atmosphere turbulence, i.e. scintillation fading with scintillation index *S.I.* as lognormal distribution, the received power will be changed to hP_t, thus BER will be given from Eqs. (2) and (6) by [4]

$$P_{e,L}(\sigma_1,\sigma_0,P_t,f_x)=\frac{1}{2}\int_{-\infty}^{\infty}f_x(X)\ erfc\left(\frac{\sqrt{2}RP_te^{2X}}{(\sigma_1+\sigma_0)}\right)dX \quad (18)$$

where $f_x(X)$ is defined by Eq. (7) and *erfc*(.) is the *complementary error function* defined as $erfc(x)=2(\pi)^{-1/2}\int_x^{\infty}\exp(-r^2)dr$. By converting the variable from *X* to *h*, the bit error rate will be presented by

$$P_{e,L}(\sigma_1,\sigma_0,P_t,\sigma_x)$$
$$=\frac{1}{\sqrt{32\pi}\sigma_x}\int_0^{\infty}\frac{1}{h}\exp\left(-\frac{\left[\ln(h)+2\sigma_x^2\right]^2}{8\sigma_x^2}\right)erfc\left(\frac{\sqrt{2}RP_th}{(\sigma_1+\sigma_0)}\right)dh \quad (19)$$

Calculation of integration (19), at times approximated, can be done by mathematical and numerical methods as follows:

A. Power Series Approach

We may rewrite the expression (19) by using (6) in the form of

$$P_{e,L}(\gamma_G,\sigma_x)$$
$$=\frac{1}{\sqrt{8\pi}\sigma_x}\int_{-\infty}^{\infty}\exp\left(-\frac{\left[X+\sigma_x^2\right]^2}{2\sigma_x^2}\right)erfc\left(\sqrt{\frac{\gamma_G}{2}}e^{2X}\right)dX \quad (20)$$

Power series representation of error function can be defined as ((13.2) in [11]),

$$erfc(x)=1-\frac{2}{\sqrt{\pi}}\sum_{k=0}^{\infty}\frac{(-1)^k x^{2k+1}}{k!(2k+1)} \quad (21)$$

then

$$erfc(\sqrt{\frac{\gamma_G}{2}}e^{2X})=1-\frac{2}{\sqrt{\pi}}\sum_{k=0}^{\infty}\frac{(-1)^k\gamma_G^{(2k+1)/2}e^{2(2k+1)X}}{2^{(2k+1)/2}k!(2k+1)} \quad (22)$$

Substituting this expression in $P_{e,L}$, it becomes

$$P_{e,L}(\gamma_G,\sigma_x)=\frac{1}{\sqrt{8\pi}\sigma_x}\int_{-\infty}^{\infty}e^{-\left(X+\sigma_x^2\right)^2/2\sigma_x^2}dX$$
$$-\frac{1}{\sqrt{2}\pi\sigma_x}\sum_{k=0}^{\infty}\frac{(-1)^k\gamma_G^{(2k+1)/2}}{2^{(2k+1)/2}k!(2k+1)}\int_{-\infty}^{\infty}e^{-\left(X+\sigma_x^2\right)^2/2\sigma_x^2}e^{2(2k+1)X}dX \quad (23)$$

The aforementioned integrals can be manipulated as

$$P_{e,L}(\gamma_G,\sigma_x)=\frac{1}{\sqrt{8\pi}\sigma_x}\int_0^{\infty}e^{-\left(X-\sigma_x^2\right)^2/2\sigma_x^2}dX \quad (24)$$
$$+\frac{1}{\sqrt{8\pi}\sigma_x}\int_0^{\infty}e^{-\left(X+\sigma_x^2\right)^2/2\sigma_x^2}dX$$
$$-\frac{1}{\sqrt{2}\pi\sigma_x}\sum_{k=0}^{\infty}\frac{(-1)^k\gamma_G^{(2k+1)/2}}{2^{(2k+1)/2}k!(2k+1)}\int_0^{\infty}e^{-\left(X-\sigma_x^2\right)^2/2\sigma_x^2}e^{-2(2k+1)X}dX$$
$$-\frac{1}{\sqrt{2}\pi\sigma_x}\sum_{k=0}^{\infty}\frac{(-1)^k\gamma_G^{(2k+1)/2}}{2^{(2k+1)/2}k!(2k+1)}\int_0^{\infty}e^{-\left(X+\sigma_x^2\right)^2/2\sigma_x^2}e^{2(2k+1)X}dX$$

It can be shown that

$$\int_0^{\infty}e^{-\left(X\pm\sigma_x^2\right)^2/2\sigma_x^2}dX=\frac{\sqrt{2\pi}\sigma_x}{2}erfc\left(\pm\frac{\sigma_x}{\sqrt{2}}\right) \quad (25)$$

and

$$\int_0^{\infty}e^{-\left(X\pm\sigma_x^2\right)^2/2\sigma_x^2}e^{\mp2(2k+1)X}dX$$
$$=\sqrt{\frac{\pi\sigma_x^2}{2}}e^{-\sigma_x/2}erfcx\left(\frac{(\pm4k\pm1)\sigma_x}{\sqrt{2}}\right) \quad (26)$$

where *erfcx*(*x*) is the *scaled complementary error function* given by

$$erfcx(x)=e^{x^2}erfc(x)=2e^{x^2}(\pi)^{-1/2}\int_x^{\infty}\exp(-r^2)dr \quad (27)$$

However, we know that *erfc*(*x*)+*erfc*(-*x*)=2, and then *erfcx*(*x*)+*erfcx*(-*x*)= $2e^{x^2}$. Finally the BER of a log-normal fading channel can be summarized as

$$P_{e,L}(\gamma_G,\sigma_x)=\frac{1}{2}$$
$$-\frac{1}{\sqrt{\pi}}e^{-\sigma_x/2}\sum_{k=0}^{\infty}\frac{(-1)^k\gamma_G^{(2k+1)/2}}{2^{(2k+1)/2}(2k+1)k!}\exp\left(\frac{(4k+1)\sigma_x}{\sqrt{2}}\right)^2 \quad (28)$$

Unlike earlier expressions, this is not approximated and not involved with zeros and weight factors regarding Hermite polynomial. This approach is investigated in the following section. However, a problem exists with expression (28), as it doesn't converge for small values of *k*. Evaluating numerically by simulation, Fig. 1 shows the BER probability by (28), $P_{e,L}$, versus averaged signal-to-noise ratio, γ_G, for different values of fading intensity, σ_x.

B. Gauss-Hermite Quadrature Approach

A general solution for numerical calculation of the integrals in the form of $\int_{-\infty}^{\infty}e^{-x^2}f(x)dx$ is presented in [12, 25.4.46], which is

$$\int_{-\infty}^{\infty} e^{-x^2} f(x)dx = \sum_{i=1}^{n} w_i f(x_i) + R_n \quad (29)$$

where n is the number of sample points used for approximation. The x_i are the roots of the Hermite polynomial $H_n(x)$ (i = 1,2,...,n); the associated weights w_i are given by $2^{n-1} n! \sqrt{\pi} / n^2 H_{n-1}^2(x_i)$; and R_n is the reminder given by $f^{(2n)}(\xi) n! \sqrt{\pi} / 2^n (2n)!$. Note that $f^{(2n)}$ is the $2n$-*th* derivative of f, and ξ is some number between -∞ and ∞. Although, in general, the precise value of R_n is unknown, its analytical form usually is known and can be used to determine an upper bound to $|R_n|$ in terms of n [11]. Abramowitz *et al.* [12, table 25.10] offers a table of abscissas and weights up to n=20. Using this equation, the BER can be approximated by

$$P_{e,L,n}(\gamma_G, \sigma_x) \approx \frac{1}{2\sqrt{\pi}} \sum_{i=1}^{n} w_i \, erfc\left(\sqrt{\frac{\gamma_G}{2} e^{2\sqrt{2}\sigma_x x_i - 2\sigma_x^2}} \right) \quad (30)$$

IV. Numerical Simulation

In this section we provide the numerical simulation of a typical fading system and provide the analysis of mathematical computations in the Section III. Evaluating numerically by simulation, Fig. 1 shows the bit error rate probability by (30), $P_{e,L}$, versus signal to noise ratio, γ_G, for different values of fading intensity, σ_x. The comparison to BER of a Gaussian channel is also shown in this figure.

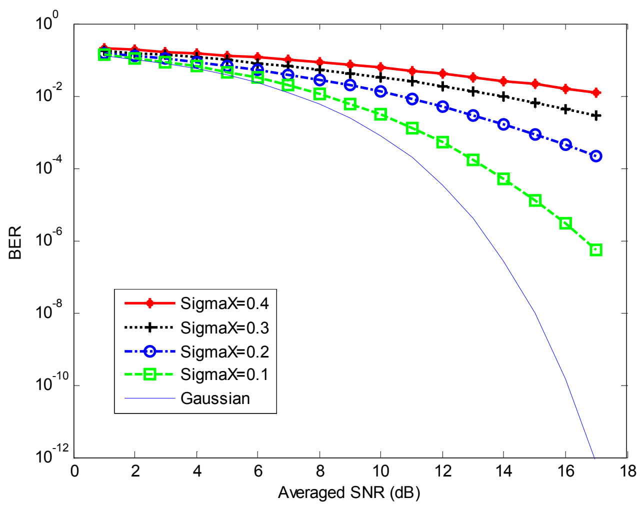

Fig. 1: The bit error probability of lognormal channel with CSI versus SNR for different value of fading intensity. The BER of a Gaussian channel (no fading) is also shown to demonstrate performance loss in a fading channel.

The BER of a Gauss–Hermite quadrature-based expression is numerically plotted in Fig. 2. The reminder R_n is illustrated in Figs. 3 and 4, for different values of fading intensity σ_x and order n. The approximation error (i.e., $\left| P_{e,L,n} - P_{e,L} \right| / P_{e,L}$), which is the normalized representation of R_n, is also illustrated in Fig. 5. Increasing the SNR does not usually decrease the approximation error. But when the fading intensity σ_x decreases, a decrease of approximation error takes place. We can observe that the approximation error has some local minimum points for almost all of the three values of n at different values of σ_x. The approximation error for the local minimum points is zero. However it does not show a zero value in Fig. 5 due to limitation of computer simulations. Above analysis was achieved with the assumption that not only the receiver knows channel model, fading distribution, fading correlation and noise statistics, but also the instantaneous CSI is available. However, the CSI information of the channel is not easily available at the receiver. The case that the receiver has no knowledge of the instantaneous fading state will be discussed in a future work by the authors.

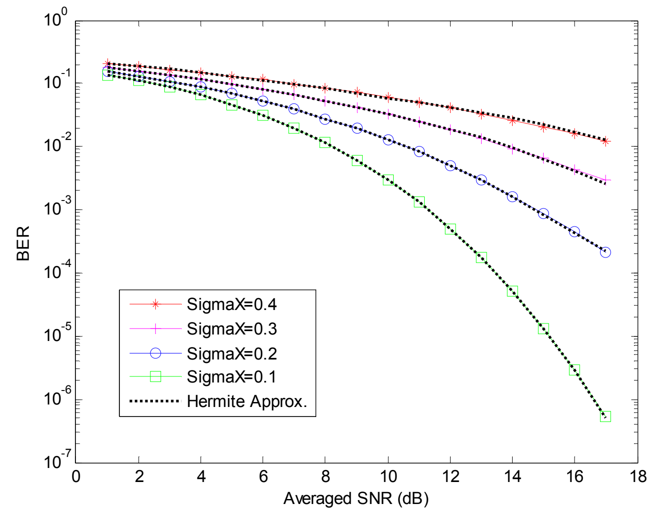

Fig 2: The Hermite-approximated probability of error for polynomial order n=5 and different values of fading intensity σ_x.

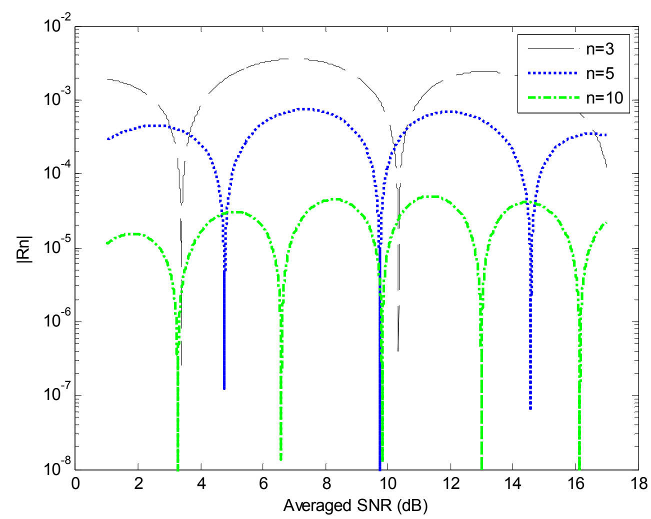

Fig 3: The reminder R_n from Hermite-approximated probability of error for different approximation polynomial orders n while $\sigma_x = 0.3$.

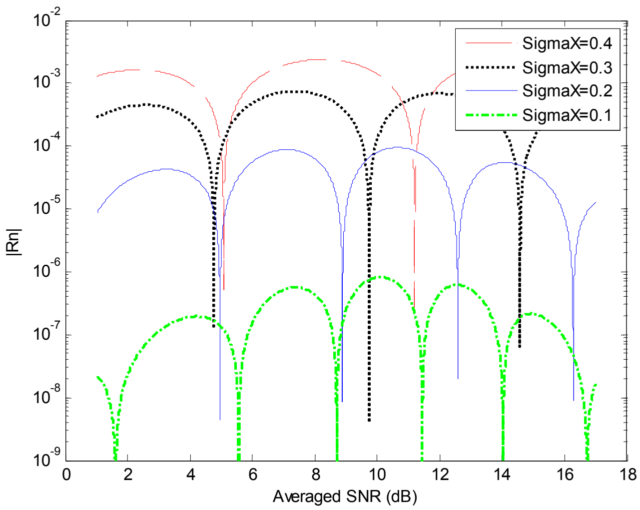

Fig 4: The reminder R_n from Hermite-approximated probability of error for polynomial order n=5 and different values of fading intensity σ_x .

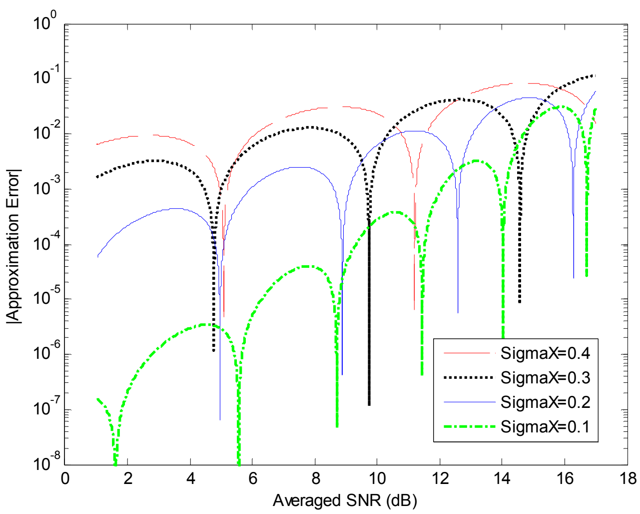

Fig 5: The approximation error of Hermite-approximated probability of error for polynomial order n=5 and different values of fading intensity σ_x .

V. CONCLUSIONS

This paper has investigated the BER analysis of a lognormally faded channel when perfect CSI is available at the receiver. In this case, although the complexity of designing the receiver will be minimized when an optimal detection is required, the BER is still under the effect of the fading. However, the receiver knows the exact value of channel coefficients at different time. A new closed-form expression employing power series was derived in this paper. We also analyzed the approximation error when a Gauss-Hermite Quadrature is used as the second approach for calculation of BER. We saw that even with a value of Hermite polynomial order n=3, the maximum of error is 5×10^{-2} for $\sigma_x = 0.3$. Also, increasing the SNR does not decrease the approximation error while decreasing the fading intensity decreases the error. Thus the normalized approximation error increases while the SNR increases and/or the fading intensity increases.

VI. ACKNOWLEDGMENTS

This work is funded by NSF grant number NSF-ECCS 0725801.

REFERENCES

[1] Gagliardi, R. M., and Karp, S., *Optical Communications*, 2nd edition, John Wiley & Sons, Inc., 1995.

[2] Kim, I. I., and Korevaar, E., Availability of Free Space Optics (FSO) and Hybrid FSO/RF Systems, *SPIE*, Vol. 4530, pp. 84-95, Aug. 2001.

[3] Harris, A., Sluss, J. J., Refai, H. H., and LoPresti, P. G., Free-space optical wavelength diversity scheme for fog mitigation in a ground-to-unmannedaerial-vehicle communications link, *Journal of Optical Engineering*, Vol. 45, p.p. 1-12, 2006.

[4] Navidpour, S. M., Uysal, M., and Kavehrad, M., BER Performance of Free-Space Optical Transmission with Spatial Diversity, *IEEE Trans. Wireless Comm.*, Vol. 6, No. 8, pp. 2813-2819, Aug. 2007.

[5] Tsiftsis, T. A., Sandalidis, H.G., Karagiannidis, G. K., and Uysal, M., Optical wireless links with spatial diversity over strong atmospheric turbulence channels, *IEEE Trans. Wireless Comm.*, Vol. 8, Issue 2, pp. 951-957, Feb. 2009.

[6] Bayaki, E., Schober, R., and Mallik, R.K., Performance analysis of MIMO free-space optical systems in gamma-gamma fading, *IEEE Trans. Comm.*, Vol. 57, Issue 11, pp. 3415-3424, Nov. 2009.

[7] Navidpour, S. M., Uysal, M., and Li, J., Analysis of coded wireless optical communications under correlated gamma-gamma channels, IEEE VTC'04, p.p. 827-931, 2004.

[8] Riediger, M. L. B, Schober, R., and Lampe, L., Multiple-Symbol Detection for Photon-Counting MIMO Free-Space Optical Communications, *IEEE Trans. Wireless Comm.*, Vol. 7, No. 12, Dec. 2008.

[9] Moradi, H., Refai, H. H., LoPresti, P. G., Atiquzzaman, M., An Estimation-Based Optimum Receiver for Free Space Optics Using Pilot-Aided Modulation, *SPIE Photonics West,* 2010.

[10] Letzepis, N., Holland, I., and Cowley, W. The Gaussian free space optical MIMO channel with Q-ary pulse position modulation, *IEEE Trans. Wireless Comm.*, Vol. 7, Issue 5, Part 1, pp. 1744 – 1753, 2008.

[11] Jeffrey, A., *Handbook of Mathematical Formulas and Integrals*, 2nd edition, Academic Press, 2000.

[12] Abramowitz, M. and Stegun, I. A., *Handbook of Mathematical Functions with Formulas, Graphs, and Mathematical Tables*, US Department of Commerce, 1964.